

# Flux transitions in a superconducting ring

Jorge Berger

Department of Sciences, Or Braude College, P.O. Box 78, 21982 Karmiel, Israel and  
Department of Physics, Technion, 32000 Haifa, Israel

We perform a numerical study of the flux transitions in a superconducting ring at fixed temperature, while the applied field is swept at an ideally slow rate. The current around the ring and its free energy are evaluated. We partially explain some of the known experimental features, and predict a considerably large new feature: in the vicinity of a critical field, giant jumps are expected.

PACS numbers: 74.25.Dw, 74.20.De, 74.60.Ec, 74.76.Db

## I. INTRODUCTION

We consider a ring of superconducting material embedded in a homogeneous magnetic field. Initially the field is too high to support a superconducting state, but it is very slowly lowered to zero while the temperature is kept constant; the field is then reversed and increased until superconductivity is destroyed. Experiments like this were performed long ago, but modern versions of it are still giving new results.<sup>1,2,3</sup> Situations similar to that considered here have been reported in Refs. 4,5. Similar experiments for weakly connected rings,<sup>6</sup> for disks<sup>7,8,9</sup> and for slabs<sup>10,11</sup> have also been widely studied.

The most prominent feature of these experiments comes from the thermodynamic need for a winding number (number of fluxoids) which is not too far from the applied flux, together with the constraint that this number has to be integer. These coupled requirements usually lead to jumps in the winding number and, accordingly, in quantities such as the current around the ring.

We consider a ring with perfect axial symmetry and analyze it by means of the Ginzburg-Landau model. We assume that the ring is very thin compared with the magnetic penetration length. Under these assumptions the free energy is (up to unimportant constants)

$$G = \int_0^{Z_2} \int_{R_i}^{Z_R} dr \left( \frac{1}{2} j^2 + \frac{1}{2} j^4 \right) + j(iR r - br = R) j^2 \quad (1)$$

where  $r$  and  $z$  are cylindrical coordinates,  $j$  is a normalized order parameter,  $R_i$  and  $R$  are the inner and outer radii of the ring,  $b = (R =)^2$  is a function of the temperature ( $\lambda$  is the coherence length) and  $b = R^2 H_e = 0$ , where  $H_e$  is the magnetic field and  $\hbar$  the quantum of flux.

## II. THE ONSET OF SUPERCONDUCTIVITY

At the onset of superconductivity the Ginzburg-Landau equations are linearized, and the case of the ring can be solved exactly.<sup>12,13,14</sup> The purpose of the present section is to point out that there exists a critical point in the normal/superconducting boundary. As will be seen

in the following sections, it appears that this critical point plays a major role in the "superheating" stability of the superconducting states. Figure 1 shows the normalized field  $b$  at which a ring with  $R_i = 0.8R$  becomes superconducting, as a function of the winding number  $m$ , for  $\lambda = 92$  and  $b = 94$ . Only integer values of  $m$  are meaningful, and only the value of  $m$  with the highest  $b$  is physically realized, but these curves are useful for explanatory purposes. We found that for  $m < 92$  these onset curves have only one maximum, whereas for  $m > 94$  they have two. At  $m = 93; b = 68$ ;  $m = 94; b = 87$  there is a critical point, where the first and the second derivative of the onset field (or of the free energy) with respect to  $m$ , both vanish. The influence of this critical point is felt quite far from its immediate vicinity. The dashed line in Fig. 1 is a line of constant (negative) free energy for  $\lambda = 110$ . We see in its upper part that for a range of about 8 winding numbers the slope of  $b$  with respect to  $m$  expressed in "natural" units, is less than a tenth. Accordingly, the free energy also has a very weak dependence on the winding number, leading to the possibility of transitions that change  $m$  by a big amount.

This critical point can be associated to two phenomena which have been discussed in the literature. The first is the condition for the formation of vortices in a slab parallel to the magnetic field.<sup>15,16,17</sup> Using the value  $0.2R$  as the thickness of the slab, the onset for the appearance of vortices is located at  $b = 81$ , not far from the critical point in our case. We can therefore expect that for  $b$  above the critical point (low temperatures) there will be vortices in the ring, whereas for small  $b$  the winding number for the inner or the outer boundary of the ring will be the same.

An additional feature noted in Ref. 15 is the crossover from a regime in which at the N-S boundary  $b = 1^{1/2}$  to a regime where  $b = 1$ . In the case of rings, this crossover applies to the background line of this boundary, which has the Little-Parks oscillations superimposed on it.<sup>14,18</sup> This is actually a dimensional crossover: at low fields the sample behaves as a thin slab and  $b = 5(3)^{1/2}$ ; at high fields it behaves as half a plane and  $b = 0.847$ . Again, the crossover occurs at  $b = 100$ .

Figure 2 shows the values of  $m$  and  $b$  at which the critical point occurs, as functions of the ratio  $R_i/R$ . Since to a rough approximation these values are inversely pro-

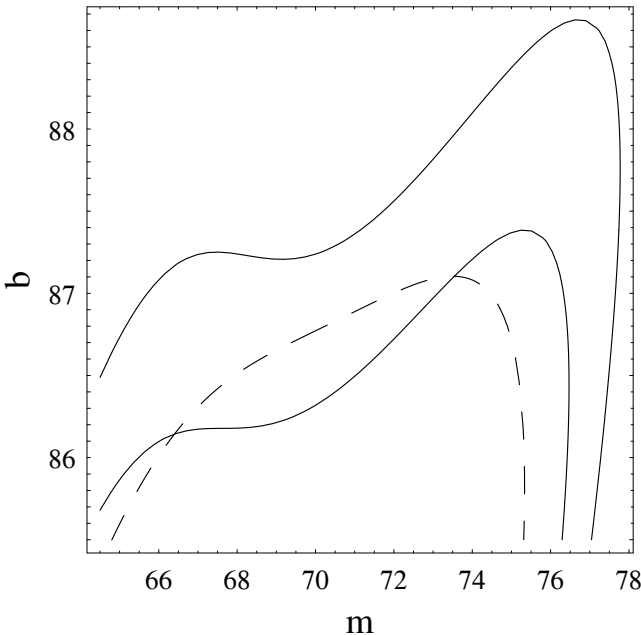


FIG. 1: The continuous lines mark the onset of superconductivity in the  $b$  versus  $m$  plane. The ring is superconducting "inside" the appropriate line. Only integer values of  $m$  are meaningful. The ratio between the inner and the outer radius is 0.8. The lower line is for  $\mu = 92$  and the upper line, for  $\mu = 94$ . The dashed line is a line of constant energy for  $\mu = 110$ . The continuous lines were obtained by an exact calculation; the evaluation of the dashed line approximates the radial dependence of the order parameter by a sum of three orthogonal polynomials.

proportional to the square of the width of the ring, the normalized values  $(1 - R_i/R)^2$  and  $b(1 - R_i/R)^2$  appear in the figure. In the following sections we will always take  $R_i = 0.8R$ , which is a representative experimental value.

### III. MATHEMATICAL METHOD

We write the order parameter as a function of the cylindrical coordinates  $r$  and  $\theta$  and assume that the ring is so thin that there is no  $z$ -dependence. We expand

$$\chi(r, \theta) = \sum_{m=-\infty}^{\infty} R_m(r) e^{im\theta}; \quad (2a)$$

$$R_m(r) = \sum_{n=0}^{\infty} c_{mn} P_n(r); \quad (2b)$$

where Eq. (2a) is a Fourier expansion and Eq. (2b) an expansion into orthogonal polynomials, with  $P_n^0(R_i) = P_n^0(R) = 0$  and such that  $P_n(r)$  vanishes  $n$  times in the range  $R_i \leq r \leq R$ . We then keep up to four terms in Eq. (2a): two "leading" terms with winding numbers  $m_0$  and  $m_1$ , and two "satellite" terms, with winding numbers  $2m_0 - m_1$  and  $2m_1 - m_0$ . In Eq. (2b) we keep the terms  $n = 0, 1, 2$  for the leading terms, and only the term  $n = 0$

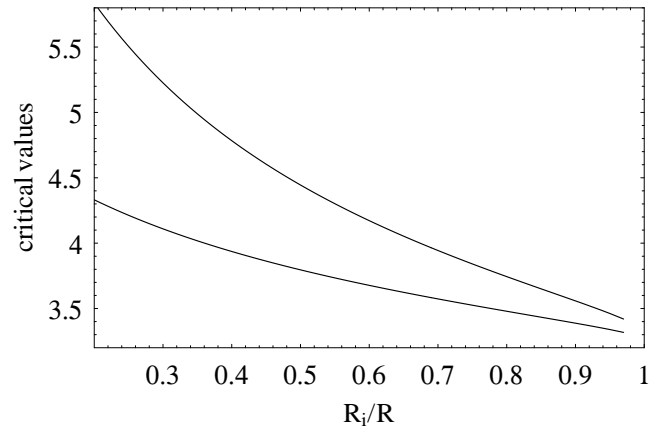


FIG. 2: Normalized values of  $\mu$  and  $b$  at which the critical point occurs, as functions of the ratio between the inner and the outer radius of the ring. The upper curve is  $(1 - R_i/R)^2$  and the lower curve is  $b(1 - R_i/R)^2$ . In the calculation of these curves we have approximated the radial dependence of the order parameter by a sum of three orthogonal polynomials.

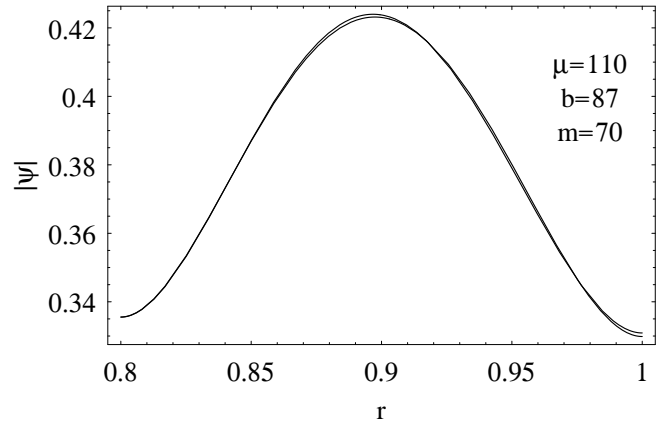


FIG. 3: Comparison of approximated and exact values of the order parameter, for a typical situation. The difference between both curves does not exceed 0.001.

for the satellite terms. The coefficients  $c_{mn}$  which are not declared to vanish, are found by minimizing the free energy. According to our results, these approximations seem to be reasonable as long as  $m$  is not much higher than that of the critical point discussed in Sec. II. The usual situation is that the weight of the leading terms is much greater than that of the satellites. In Fig. 3 we compare the radial dependence of an axially symmetric order parameter obtained by the present approximations to that from an exact calculation.

Our procedure is as follows. For fixed temperature ( $\mu$  fixed), we evaluate the magnetic field for the onset of superconductivity. At the onset, the Ginzburg-Landau equations are linear, so that the order parameter has axial symmetry and the sum (2a) contains only one  $m$ , which we denote by  $m_0$ . The field is then gradually lowered and for every field we evaluate the order parameter

$R_{m_0}(r)e^{m_0i}$ . We then check the stability of this order parameter against small variations which contain the winding numbers  $m_0$  and  $m_0 + 1$ , where  $1$  is swept over at least the range  $1 \leq 1 = 5$ . For each variation we evaluate the Hessian of the variation of the free energy and obtain its eigenvalues. If all the eigenvalues are positive, it means that  $R_{m_0}(r)e^{m_0i}$  is stable, and we proceed to decrease the field by a small step.

If any of the eigenvalues is negative, it means that  $R_{m_0}(r)e^{m_0i}$  is unstable with respect to the variation represented by the corresponding eigenstate. We denote by  $m_1 = m_0 + 1$  the value of the winding number that has the highest weight in the variation against which  $m_0$  was unstable. We now perform a minimization of the free energy over states of the form (2), where the leading winding numbers are  $m_0$  and  $m_1$ . The initial state from which the minimization flows is a combination of the former state with  $m = m_0$  and of the eigenstate that had the negative eigenvalue. The minimization may lead to a state in which only one winding number has a significant weight; in this case we recover the previous situation and we just have to update the value of  $m_0$ . The other possibility to be left with a combination of winding numbers (which means that  $j \neq j$  is not axially symmetric).

Several arbitrary decisions have to be taken when studying the decay of the state  $m = m_0$ , among them, (i) what initial weights should one give to the  $m_0$  and to the  $m_1$  states in their initial combination? (ii) which minimization method should be used? (iii) when is the weight of some winding number sufficiently small to be considered "not significant"? We have used several criteria and become convinced that, in most cases, our results do not depend on the particular choices.

If the order parameter is of the form (2a) with leading winding numbers  $m_0$  and  $m_1$ , we check its stability along similar lines to those described for a symmetric case. This time the attempted variations contain combinations of winding numbers  $1, 2m_0 + 1$  and  $2m_1 + 1$ , where  $1$  is swept over at least the range  $\max(m_0, m_1) \leq 1 \leq \max(m_0, m_1) + 1$ .

For each field, after the order parameter is known, the normalized current density is evaluated as  $\text{Re}[(iR r \text{br} = R^2)]$  and then the current (per unit height) is obtained by integration of the tangential component over  $r$ .

## IV. RESULTS

### A. Near $T_c$

Figure 4 shows the current around the ring, as a function of the field, for low values of  $\beta$ . As expected, there are discontinuities in the current, nearly periodically spaced. These discontinuities correspond to the passage between consecutive winding numbers.

For  $\beta = 0.475$  and close to  $b = -4.35$ , the ring is in the normal state. This reentrant behavior is due

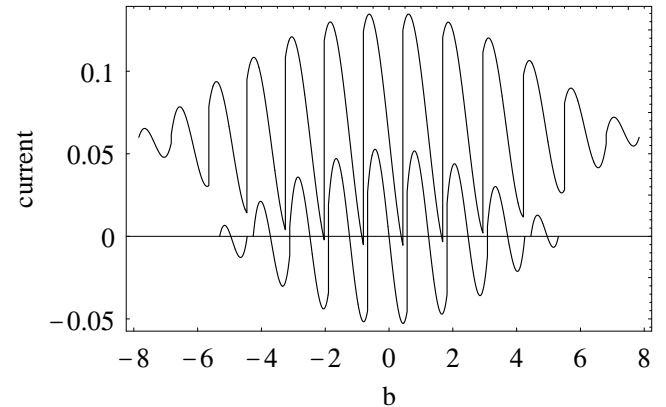


FIG. 4: Normalized current as a function of the normalized field for  $\beta = 0.475$  and for  $\beta = 0.95$ . For visibility, the curve for  $\beta = 0.95$  has been raised by 0.06. The physical current per unit height, in electrostatic units, is obtained by multiplying the normalized current by  $c_0 = 2(2\pi R)^2$ , where  $c_0$  and  $R$  are the speed of light and the Ginzburg-Landau parameter.

to the Little-Parks oscillations. For a ring with  $R_i = 0.8R$ , reentrant superconductivity is possible in the range  $0.02 \leq \beta \leq 12.4$ . For  $\beta < 0.02$ , only the Meissner state ( $m = 0$ ) exists; in the range  $0.02 \leq \beta \leq 12.4$  there are "windows" for which superconductivity is interrupted when passing from one  $m$  to the next. For low values of  $\beta$  these windows are wide, but, as  $\beta$  increases, the background slope of the N-S boundary in the  $b$  plane increases and these windows become narrower. For  $\beta > 12.4$  the N-S boundary is monotonic.

### B. Short coherence length

Figures 5 and 6 show our results in the range  $20 \leq \beta \leq 120$ . For  $\beta > 120$ , our approximation of Eq. (2a) by four uniformly spaced harmonics breaks down. Physically, this failure indicates that for  $\beta > 120$  there can be vortices in the ring which are not equidistant from the axis of the ring.

While in Fig. 4 the current is a nearly odd function of the field, indicating that hysteresis is a minor effect, in Fig. 5 the current is an almost even function, indicating that hysteresis is dominant. We observe that qualitatively different regions appear in nearly symmetric pairs. In the following, we shall review these regions, by decreasing values of  $\beta$ .

#### 1. Near the onset

Figures 7 and 8 show our results for high values of  $\beta$ , with  $\beta = 110, 120$  or  $130$ . Near the onset of superconductivity, the approximation of the expansion (2a) by a limited number of terms remains valid beyond  $\beta = 120$ . The region at the right consists of steps where a single

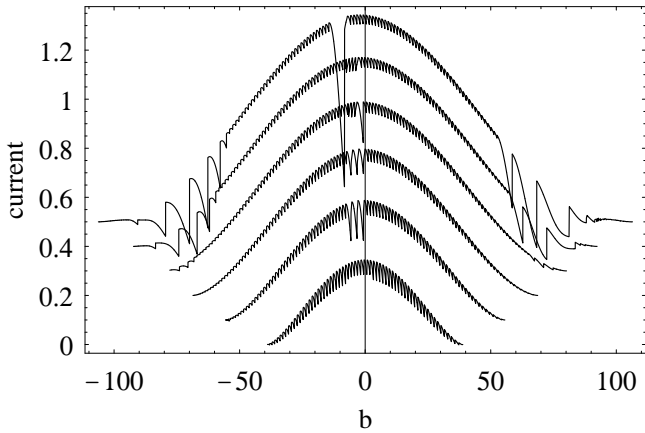


FIG . 5: Normalized current as a function of the normalized field for  $m = 20, 40, 60, 80, 100, 120$ . The lowest line is for  $m = 20$  and the highest for  $m = 120$ . Shifts of 0.1 have been inserted between consecutive lines.

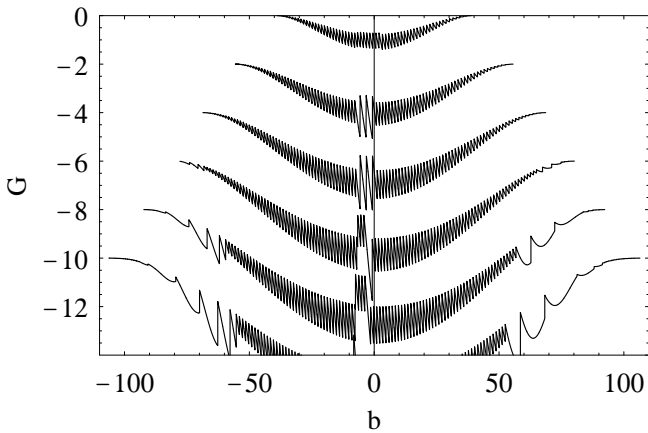


FIG . 6: Free energy as a function of the normalized field for  $m = 20, 40, 60, 80, 100, 120$ . The highest line is for  $m = 20$  and the lowest for  $m = 120$ . Shifts of 2 have been inserted between consecutive lines. The central part of  $m = 120$  has been chopped.

value of  $m$  is left in (2a) and, as  $b$  is lowered,  $m$  decreases by 1 between consecutive steps. There are five such steps for  $m = 120$  and 130, and four steps for  $m = 110$ . The current always drops when the state decays to a lower  $m$ .

## 2. Breaking of axial symmetry

This is roughly the region  $87 < b < 94$  for  $m = 110$ ,  $81 + 7 < b < 94 + 7$  for  $m = 120$  and includes most of the line for  $m = 130$  in Fig. 7. If we denote by  $(m_0)$  a state with a single harmonic  $m = m_0$  and by  $(m_0; m_1)$  a state with two leading winding numbers  $m_0$  and  $m_1$ , this region extends from  $(84; 70)$  to  $(77; 65)$  for  $m = 110$ , from  $(91; 74)$  to  $(78; 66)$  for  $m = 120$  and from  $(98; 79)$  to an uncalculated state for  $m = 130$ .

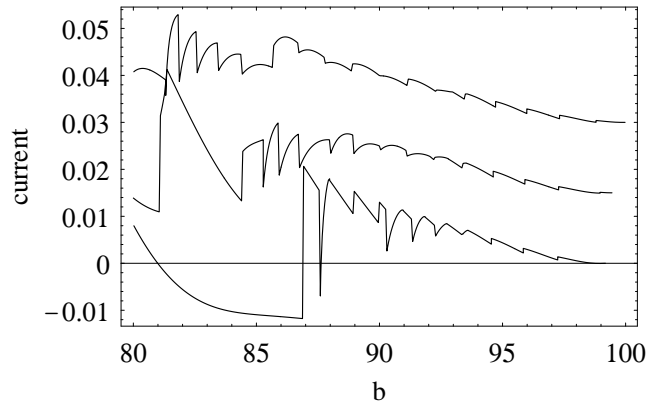


FIG . 7: Normalized current near the onset of superconductivity. The lowest line is for  $m = 110$  and sits at its true position. The other lines are for  $m = 120$  and  $m = 130$ . For each increment of 10, the position of the line is raised by 0.015 and is also shifted by 7 to the left.

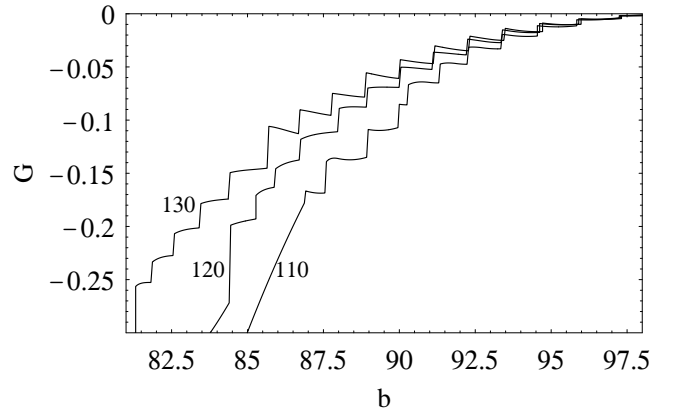


FIG . 8: Free energy near the onset of superconductivity. The steepest line is for  $m = 110$  and sits at its true position. The other lines are for  $m = 120$  and  $m = 130$ . For each increment of 10, the position of the line is shifted by 7 to the left.

We may divide this region into a subregion of "incipient symmetry breaking" and a subregion of "developed symmetry breaking". The subregion of incipient symmetry breaking consists of the sequence of double steps  $(m_0^{(1)}) \rightarrow (m_0^{(1)}; m_1^{(1)}) \rightarrow (m_0^{(2)}) \rightarrow (m_0^{(2)}; m_1^{(2)})$ . Here  $m_0^{(i+1)} = m_0^{(i)} - 1 > m_1^{(i)}$ , so that the transitions  $(m_0^{(i)}; m_1^{(i)}) \rightarrow (m_0^{(i+1)})$  are discontinuous; on the other hand, the transitions  $(m_0^{(i)}) \rightarrow (m_0^{(i)}; m_1^{(i)})$  are continuous bifurcations. In the subregion of developed symmetry breaking, all the states are combinations with two leading winding numbers. For  $m = 130$  there is only one step with incipient symmetry breaking and for  $m = 120$  there are two steps; for  $m = 110$ , incipient symmetry breaking extends over the entire region. Some segments are very short, and cannot be seen in the graph.

The subregion of developed symmetry breaking can be subdivided further: in its high-eld part the transitions

TABLE I: Fluxoid numbers occurring in the critical region. Negative numbers are for the region in the negative field.

states	
120	(61) ! (53) ! (48)
120	(39) ! (41) ! (45) !
	(51) ! (59) ! (69) ! (79)
110	(66) ! (57) ! (51) ! (48)
100	(74) ! (64) ! (56) ! (51)
100	(43) ! (45) ! (49) ! (55) ! (63) ! (72)
95	(75) ! (65) ! (58) ! (53) ! (51)
90	(72) ! (64) ! (57) ! (53)
80	(65) ! (62) ! (59) ! (57)
80	(51) ! (53) ! (56) ! (60) ! (64)

$(m_0^{(i)}; m_1^{(i)})$  !  $(m_0^{(i+1)}; m_1^{(i+1)})$  have either  $m_0^{(i+1)} = m_0^{(i)}$  or  $m_1^{(i+1)} = m_1^{(i)}$ ; for lower fields there may be "cascades". By a cascade we mean that, after a state decays, the new state is already unstable with respect to a third state, and decays at the same field at which it appeared. By means of cascades,  $m_0$  and  $m_1$  can both change simultaneously.

For axially symmetric states, the slope of the current in Fig. 7 is negative. On the other hand, for combinations with two leading winding numbers, the current is a markedly convex function, and can reach large positive slopes. For decays that follow after these large positive slopes, the current usually rises.

### 3. Critical region

This is the region with large discontinuities near  $b=70$ . For  $b=120$  and  $b=110$  the region of asymmetry ends with a long cascade, the last stage of which is a discontinuous decay into a symmetric state. For  $b=100$  the region of asymmetry is absent. For  $b=100$  the critical region begins with a decay in which  $m$  overshoots and then goes up. For  $b < 0$ , the critical region in which  $m$  jumps by several units appears without previous signs.

Table I is a record of the states through which the critical region passes.

One notices that for  $b > 0$  the number of fluxoids that go through the ring during the critical region is largest for  $b$  near its critical value. The largest signal in the current-field graph, as well as the number of fluxoids that go through for  $b < 0$ , appear to be at higher values of  $b$ .

### 4. Subcritical region

This is the broadest region in Figs. 5 and 6. As the field decreases through the critical region, jumps in the winding number decrease from giant to moderate, until

we finally reach a region in which the winding number changes by just one in each decay. For  $b=60$  the two previous regions are absent and there is no distinction between this and the first region.

For  $20 \leq b \leq 60$  and  $b > 0$ , the average range  $b$  between consecutive jumps in this region is 1.30; for  $b < 0$ ,  $b = 1.17$ . This difference can be understood, since for  $b > 0$  a delay in the decays is produced by "supercooling" and in the negative region it is necessary to catch up with this delay. For  $80 \leq b \leq 120$ ,  $b = 1.24$  for positive fields and  $b = 1.23$  for  $b < 0$ , indicating that the presence of the critical region helps to release most of this delay. Note that  $b$  is not close to unity due to our choice of the outer radius as the unit of length. Had we chosen the average radius  $0.9R$  as the unit of length (as in Ref. 1), we would have had to divide the values of  $b$  by  $1=0.9^2 = 1.235$ .

### 5. Low fields

This is a short region centered at slightly negative fields. In this region the "satellite" harmonic  $2m_1 - m_0$  is not necessarily small. In this region the results we obtain are sensitive to the minimization strategy, and the results in Figs. 5 and 6 are less reliable here than in the other regions.

## V. COMPARISON WITH EXPERIMENTS

To our knowledge, the experiments closest to the situation discussed in this article are Ref. 1 and Ref. 3. Reference 1 deals with only three fluxoids, and from the present point of view may be considered featureless. (See however Ref. 19.)

Reference 3 reports on two rings. In both cases the estimated mean radius is 2.16 m and the coherence length, 180 nm. For their wide ring,  $R = R_i = 630$  nm. Using graph 2, these values result in  $b = (R =)^2 = 3$  crit, far beyond the region we have studied. One observation can nevertheless be ventured: the critical value of the field is  $b_{\text{crit}} = 56$ , which for this geometry corresponds to about 60 G. The "catastrophic behavior" in their Fig. 5 begins not far from there.

Their narrow ring has a width  $R = R_i = 316$  nm, which now implies  $b = (R =)^2 = 0.9$  crit. Translated to our case, this corresponds to  $b = 80$ . Inspection of their Fig. 2 and our Fig. 5 suggests that  $b = 60$  would give a better comparison. The difference between  $b = 80$  and  $b = 60$  could be due to a 15% error in any of the reported lengths, and is an expected experimental uncertainty. There are some similar features between our results and the experimental curve: there is a central region sandwiched between two outer regions, like the low-

field and the subcritical regions of the previous section. The size of the discontinuities grows towards lower fields at an apparently correct pace. The average period  $b$  for positive fields is longer than that for negative fields,

and the ratio 1:30 :1:17 seems to be of the right order. For  $a = 60$  and  $b = 0$  we predict a current of the order of  $0.6c_0 t = 2(2\pi R)^2$ , where  $t$  is the thickness of the ring. Assuming  $t = 90\text{nm}$  and  $c_0 = 0.5$ , this current amounts to  $2 \times 10^6 \text{ esu/sec}$ . A current like this would induce a magnetic field of  $2\text{G}$  at the center of the ring; this is the correct order of magnitude.

However, the range of the central part is much wider than predicted. In view of this discrepancy, we ought to revise our idealizations.

We have neglected the induced field. The magnetic penetration depth  $\lambda = R^{1/2} = 0.5 \times 2300\text{nm} = 60^{1/2} \times 150\text{nm}$  is only marginally larger than the thickness of the ring, so that our assumption is not clearly justified. The influence of the induced field on "superheating" for the case of thick disks has been considered in Ref. 20 and does not hint at a qualitatively different behavior.

An experimental ring never has perfect axial symmetry. This in-

try. This imperfection has been treated in previous studies<sup>21,22</sup> and has a profound influence near the onset of superconductivity, but is not expected to be important deep inside the superconducting region. In the present problem, variation of the width with the height might also be important.

Decays most probably occur before the ideal metastability limit is reached, mainly due to electromagnetic noise. When taking measurements, noise can be filtered out by a lock-in amplifier, but in order to avoid premature decays only shielding could help.

#### Acknowledgments

This article has benefited from comments raised by A. G. Ein, O. M. Egger, S. Pedersen and J. Rubinstein.

---

Electronic address: phr76j@tx.technion.ac.il

- <sup>1</sup> X. Zhang and J. C. Price, Phys. Rev. B 55, 3128 (1997).
- <sup>2</sup> A. Kanda, M. C. Geisler, K. Ishibashi, Y. Aoyagi, and T. Sugano, Physica B 284, 1870 (2000).
- <sup>3</sup> S. Pedersen, G. R. Kofod, J. C. Hollingbery, C. B. Sørensen, and P. E. Lindelof, Phys. Rev. B 64, 104522 (2001).
- <sup>4</sup> A. Bezryadin, A. Buzdin, and B. Pannetier, Phys. Rev. B 51, 3718 (1995).
- <sup>5</sup> B. J. Baelus, F. M. Peeters, and V. A. Schweigert, Phys. Rev. B 61, 9734 (2000).
- <sup>6</sup> A. H. Silver and J. E. Zimmerman, Phys. Rev. 157, 317 (1967).
- <sup>7</sup> A. K. Geim, I. V. Grigorieva, S. V. Dubonos, J. G. S. Lok, J. C. Maan, A. E. Filippov, and F. M. Peeters, Nature 390, 259 (1997).
- <sup>8</sup> H. J. Fink and A. G. Pesson, Phys. Rev. 168, 399 (1968).
- <sup>9</sup> V. A. Schweigert, F. M. Peeters, and P. S. Deo, Phys. Rev. Lett. 81, 2783 (1998).
- <sup>10</sup> J. Guimbel, L. Civale, F. de la Cruz, J. M. Marduck, and

- I. K. Schuller, Phys. Rev. B 38, 2342 (1988).
- <sup>11</sup> C. Bolech, G. C. Buscaglia, and A. Lopez, Phys. Rev. B 52, 15719 (1995).
- <sup>12</sup> D. Saint-James, Phys. Lett. 15, 13 (1965).
- <sup>13</sup> R. Benoit and W. Zwerger, Z. Phys. B 103, 377 (1997).
- <sup>14</sup> V. B. Bulyndoncx, L. V. Look, M. Verschueren, and V. V. Moshchalkov, Phys. Rev. B 60, 10462 (1999).
- <sup>15</sup> D. Saint-James, G. Sama, and E. J. Thomas, Type II Superconductivity (Pergamon, New York, 1968).
- <sup>16</sup> H. A. Schultens, Z. Physik 232, 430 (1970).
- <sup>17</sup> H. J. Fink, Phys. Rev. 177, 732 (1969).
- <sup>18</sup> H. T. Jallal, J. Rubinstein, and P. Stemberg, Phys. Rev. Lett. 82, 2935 (1999).
- <sup>19</sup> J. Berger and J. Rubinstein, Phys. Rev. B, 56, 5124 (1997).
- <sup>20</sup> V. A. Schweigert and F. M. Peeters, Physica C 332, 266 (2000).
- <sup>21</sup> J. Berger and J. Rubinstein, Phys. Rev. B 59, 8896 (1999).
- <sup>22</sup> J. Berger, in Connectivity and Superconductivity, edited by J. Berger and J. Rubinstein (Springer, Heidelberg, 2000).